Catalysis Today 164 (2011) 34–39

Contents lists available at ScienceDirect

Catalysis Today

journal homepage: www.elsevier.com/locate/cattod

# Studies on oxy-bromination of methane and coke deposition over $FePO_4/SiO_2$ catalysts

Ronghe Lin[a,c], Yunjie Ding[a,b,*], Leifeng Gong[a,b], Wenda Dong[a,c], Weimiao Chen[a], Yuan Lu[a]

[a] Dalian National Laboratory for Clean Energy, Dalian Institute of Chemical Physics, Chinese Academy of Sciences, Dalian 116023, PR China
[b] State Key Laboratory of Catalysis, Dalian Institute of Chemical Physics, Chinese Academy of Sciences, Dalian 116023, PR China
[c] Graduate School of Chinese Academy of Sciences, Beijing 100049, PR China

ARTICLE INFO

*Article history:*
Available online 2 November 2010

*Keywords:*
Coke deposition
$FePO_4/SiO_2$
Methane
Oxy-bromination
Preparation method
Stability

ABSTRACT

Different $FePO_4/SiO_2$ catalysts have been synthesized and employed for the oxy-bromination of methane reaction. The long-term stability experiments and the influences of $FePO_4$ loading and reaction temperature have been investigated. It was demonstrated that the $FePO_4/SiO_2$ catalysts were very stable during 200 h time-on-stream. High total selectivity for $CH_3Br$ plus CO with equimolar ratio could be achieved by manipulating the reaction variables. However, coke deposition was found on the used catalysts after a long running period. Characterization techniques such as $N_2$-adsorption, Fourier-transform infrared spectroscopy and temperature-programmed oxidation were employed to investigate the fresh and used samples. The characterization results implied that the accumulation of $CH_2Br_2$ during the reaction could be the direct cause of coke deposition.



## 1. Introduction

Direct conversions of light alkanes in natural gas to liquids as alternative chemical feedstocks have attracted considerable attentions in this decade due to the diminishing proven reserves [1]. The current commercial technologies for natural gas utilization are dominated by an indirect route via syngas which involves the reforming of methane. However, the reforming process is highly energy-intensive, and the large investment required makes it unsuitable for use in small- and medium-scale natural gas fields [2]. It is estimated that 30–60% of natural gas reserves are classified as stranded due to the lack of infrastructure [3,4]. The development of practical technologies for the successful utilization of these resources presents a great challenge to the chemist and engineer.

Methane can be transformed into useful chemicals by two steps with the mediation of halogens. For the first step, methane halogenation reactions are thermodynamically advantageous and practical without considering the corrosion nature of halogens [5]. It has been reported that $CH_3Cl$ could be synthesized via oxy-chlorination reaction over $LaCl_3$-based catalysts, and then it was subsequently converted into olefins over ZSM-5 [6,7]. $CH_3Cl$ or $CH_3Br$ can also be produced with high selectivity by monohalogenation of methane over supported solid super-acids catalysts [8,9]. By a second process, the methyl halides can be converted to methanol, dimethyl ether or other chemicals over secondary catalysts [8,10,11]. An integrated multi-step process from methane to oxygenates and olefins has also been described by Lorkovic et al. [11–14]. However, the first step of this process involves the radical reactions between methane and bromine, limiting high selectivity to $CH_3Br$. As an improvement, Wang et al. [15–17] proposed a new process: oxy-bromination of methane (OBM), in which molecular $O_2$ and a solution of $HBr/H_2O$ were employed instead of bromine for the activation of methane. High selectivities to $CH_3Br$ were reported over Ru- and Rh-based catalysts, even though the reactions were claimed as radical reactions.

Due to the introduction of molecular $O_2$ to the OBM system, the reaction can provide versatile choices of intermediate products, such as equimolar $CH_3Br$ and CO. Previous reports proved that carbonylation of methyl halides to acetic acid were practical, especially for $CH_3Br$ [15,16,18]. It has also been revealed that $CH_3Br$ is the primary product while $CH_2Br_2$ and CO are the secondary in the OBM system [15]. While the selective mono-bromination of methane depends greatly upon electrophilic catalysts [8,9], the parallel reactions between bromo-substitution (Eq. (1)) and $CH_3Br$ oxidation (Eq. (2)) offer the advantage that simultaneous production of $CH_3Br$ and CO can be achieved easily by suppressing Eq. (1). Thus, it is feasible to provide equimolar $CH_3Br$ and CO as a potential feedstock for the production of acetic acid (Eq. (3)), as the carbonylation reaction between $CH_3Br$ and CO produced acetic acid in very high yield [16].

$$CH_3Br + Br_2 \rightarrow CH_2Br_2 + HBr \quad (1)$$

* Corresponding author at: 457 Zhongshan Road, Dalian, Liaoning 116023, China.. Tel.: +86 411 84379143; fax: +86 411 84379143.
*E-mail address:* dyj@dicp.ac.cn (Y. Ding).

0920-5861/$ – see front matter © 2010 Elsevier B.V. All rights reserved.
doi:10.1016/j.cattod.2010.09.023

$$CH_3Br + O_2 \rightarrow HBr + CO + H_2O \quad (2)$$

$$CH_3Br + CO + H_2O \rightarrow CH_3COOH + HBr \quad (3)$$

Considering the high cost and limited resources of noble metals, we have studied the OBM reaction over various silica-supported non-noble metal oxide catalysts [19,20]. It was found that $BaO/SiO_2$ showed high initial activity for the OBM reaction, but it deactivated quickly due to serious leaching of active components under strong acidic atmosphere [19]. Recently, we reported a highly efficient and stable silica-supported iron phosphate catalyst for the OBM reaction [20]. The phase evolution processes of iron phosphates and possible active sites have been illustrated by combined spectroscopic techniques, but the process conditions are not surveyed in details. Therefore, we report a thorough investigation on the effects of preparation methods and reaction variables in this work. Besides, the long-term stability experiments were carried out. Slight deactivation occurred over the catalysts due to carbon deposition. The cause of coke formation was attributed to the accumulation of $CH_2Br_2$ during the reaction.

## 2. Experimental

### 2.1. Catalyst preparation

Three different types of silica-supported $FePO_4$ samples were prepared according to the methods described below. For the first series of samples, aqueous solutions of $Fe(NO_3)_3$ and $NH_4H_2PO_4$ (P/Fe = 1.0) were mixed thoroughly at room temperature. Then, silica-gels with different weights were subject to impregnating with the mixed solution, with the nominal $FePO_4$ loading of 5, 10, 20, 30 wt.%. The derived slurries were then dried at 90 °C to evaporate the liquids, and finally calcined at 600 °C for 10 h to generate the catalysts. Specifically, the derived sample with $FePO_4$ loading of 10 wt.% was denoted as P1.

For the second sample (denoted as P2), $H_3PO_4$ was used as the precursor instead of $NH_4H_2PO_4$, and the other procedures were the same as those of P1.

The preparation of the third sample is similar to the synthesis of bulk $FePO_4$ by precipitation. Firstly, an aqueous solution of 0.5 M $Fe(NO_3)_3$ was added to an ammonia solution at constant stirring to generate FeOOH. The fresh slurry was heated slowly to 90 °C in a water bath, and then an aqueous solution of 0.5 M $H_3PO_4$ was added. After the slurry was stirred for another 1 h, silica-gel was subject to impregnating with the slurry overnight. Finally, the slurry was dried and activated as described above for P1. The derived sample was denoted as P3 (P/Fe = 1.0, 10 wt.% loading).

For comparison, a sample of 10 wt.% $Fe_2O_3/SiO_2$ was synthesized by impregnation method. To be brief, an aqueous solution of 0.5 M $Fe(NO_3)_3$ was impregnated with the silica-gel overnight. Then, it was dried at 120 °C and finally calcined at 600 °C for 10 h.

### 2.2. OBM reaction evaluation

The detailed evaluation methods of the OBM reaction have been reported in previous publications. Briefly, a catalyst of 2.0 g was loaded in the central part of a quartz-tube microreactor, with quartz beads above the catalyst bed to provide a pre-heated zone for uniform gas distribution. For each of the tests, the $HBr/H_2O$ solution was introduced to the reactor by a syringe after the temperature was above 500 °C. The sampling and analysis methods have been described in an earlier report [19].

### 2.3. Characterization of catalysts

The structural properties of the samples were determined by $N_2$-adsorption–desorption method, using a physical adsorption instrument (Quantachrome, USA). Specific surface area and pore volume were determined by $N_2$ adsorption at 77 K after samples were pretreated at 350 °C under vacuum for 3 h.

Fourier-transform infrared spectra (FTIR) were recorded with a BRUKER EQUINOX 55 Spectrometer, having a resolution of 4 $cm^{-1}$ and using the KBr disk method.

Hydrogen temperature-programmed reduction ($H_2$-TPR) measurements were carried out on a Micromeritics Autochem 2910 system equipped with a TCD detector. Ahead of each test, 100 mg of each sample was loaded in a U-type tube. Then, it was heated from room temperature to 800 °C in a flow of 10 vol.% $H_2$/Ar (50 sccm) at a ramp of 10 °C/min. Water produced during the reduction was removed by a cooling trap.

Temperature-programmed oxidation (TPO) measurement was carried out on a Micromeritics Autochem 2910 system equipped with a mass detector. Ahead of the test, 100 mg of the coked sample was loaded in a U-type tube. It was heated to 350 °C in a flow of He at a ramp of 10 °C/min and then stabilized for another 2 h. After the temperature of the sample returned to room temperature, it was heated to 900 °C in a flow of 2 vol.% $O_2$/He (30 sccm) at a ramp of 10 °C/min.

**Table 1**
Physical properties of the synthesized catalysts and P1 for different reaction times.

| Catalyst | $S_{BET}$ ($m^2$/g) | $V_{total}$ (ml/g) | Average pore size (nm) |
|---|---|---|---|
| P1 | 363 | 1.03 | 11.4 |
| P1-100 | 290 | 0.99 | 13.6 |
| P1-300 | 36 | 0.07 | 7.6 |
| P2 | 303 | 0.83 | 11.0 |
| P3 | 309 | 0.58 | 11.0 |

*Note*: P1 treated in the OBM reaction after 100 h was denoted as P1-100, and the used catalyst after regeneration and reaction for another 100 h was denoted as P1-300.

## 3. Results and discussion

### 3.1. Physicochemical properties of $FePO_4/SiO_2$ catalysts

#### 3.1.1. Structural properties of $FePO_4/SiO_2$ catalysts

The structural properties of the fresh samples were investigated by $N_2$-adsorption and FTIR techniques. The physical properties of corresponding samples are listed in Table 1. Obviously, P1 has higher surface area and larger total mesopore volume than the other two samples, and the average pore size is also a little larger for P1. P2 and P3 show similar surface areas and average pore sizes, but the mesopore volume of the latter is much smaller. The transmission IR spectra of the samples were also recorded, as presented in Fig. 1. All the samples displayed the same absorptions at the broad region between 400 and 1200 $cm^{-1}$ that are the distinctive vibrations of phosphate groups. The peak at 1638 $cm^{-1}$ corresponds to the vibrations of surface hydroxide [21]. The peaks at 1104 and 980 $cm^{-1}$ could be assigned to the symmetric stretching vibrations of $PO_3$ groups [21]. The peaks at 809 and 467 $cm^{-1}$ could be attributed to the asymmetric stretching vibrations of P–O–P groups and the bending vibrations of $PO_3$ groups, respectively [21,22]. The results from $N_2$-adsorption and FTIR demonstrated that all the synthesized samples had similar structural properties.

#### 3.1.2. Redox abilities of $FePO_4/SiO_2$ catalysts

The redox abilities of the fresh samples were studied by $H_2$-TPR technique, and the results are shown in Fig. 2. For comparison, the $H_2$-TPR profile of $Fe_2O_3/SiO_2$ was also presented in Fig. 2. P1 and P2 showed similar reduction peaks around 482 °C which could be assigned to the reduction from $FePO_4$ to $Fe_2P_2O_7$ [23]. The reduction profile of P3 is much more complicated, which showed two relatively larger reduction peaks around 452 and 790 °C and a

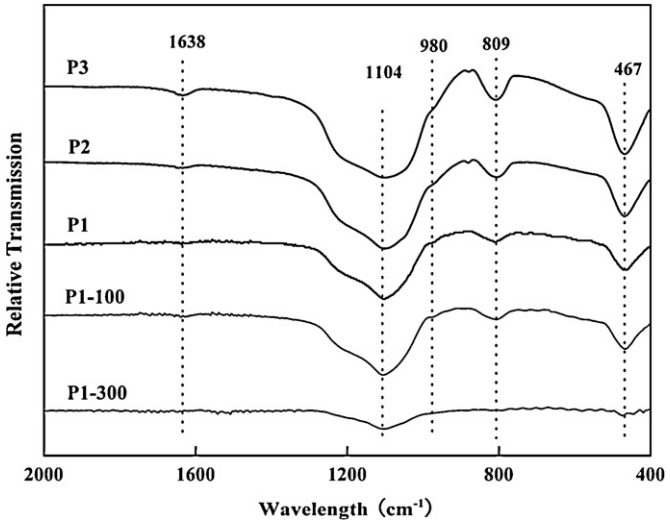


**Fig. 1.** Infrared spectra of the synthesized catalysts and P1 for different reaction times.

smaller reduction peak around 584 °C. Comparing the reduction profiles between P3 and $Fe_2O_3/SiO_2$, one might speculate that the ferric components in P3 existed as a mixture of $Fe_2O_3$ and $FePO_4$. Therefore, the first reduction peak in P3 could be a reflection of the coreduction of $Fe_2O_3$ and $FePO_4$.

### 3.2. Catalytic performances of $FePO_4/SiO_2$ catalysts

Fig. 3 shows the time-on-stream performances of the OBM reaction over different $FePO_4/SiO_2$ catalysts. In the initial stage, the reactions over all the catalysts went through apparent induction periods. During the periods, the ratio of $CH_3Br$:CO increased dramatically while the conversion of methane also showed a slight increase, especially for the first 10 h. The conversions of methane over P1 and P2 are roughly the same (about 50%), but a little lower over P3. Besides, the ratios of $CH_3Br$:CO over P1 and P2 are also very close (about 1.0), which are almost doubled as compared with the value over P3 after the reactions gradually became stable.

It should be noticed that no $CO_2$ was produced over P1 and P2 in the initial stage of the reaction, whereas it was detected immediately over P3. When the reaction time was prolonged, the $CO_2$ selectivity decreased gradually and finally dropped to zero. The $H_2$-TPR profile of P3 in Fig. 2 has suggested that $Fe_2O_3$ might be formed in this sample. Actually, $CO_2$ was also produced immediately in our test when $Fe_2O_3/SiO_2$ was used as the catalyst at similar OBM reaction conditions. Thus, it is deduced that the production of $CO_2$ over P3 was resulted from the $Fe_2O_3$ species. Obviously, the $Fe_2O_3$ in P3 could be removed largely by HBr during the reaction, leading to the decline of $CO_2$ selectivity.

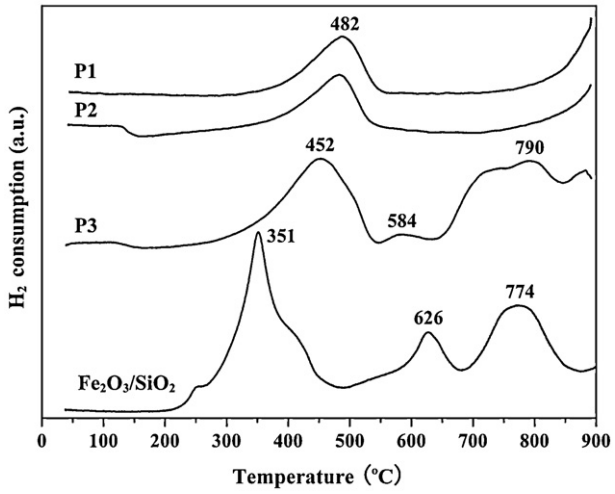


**Fig. 2.** $H_2$-TPR profiles of the synthesized catalysts and $Fe_2O_3/SiO_2$.

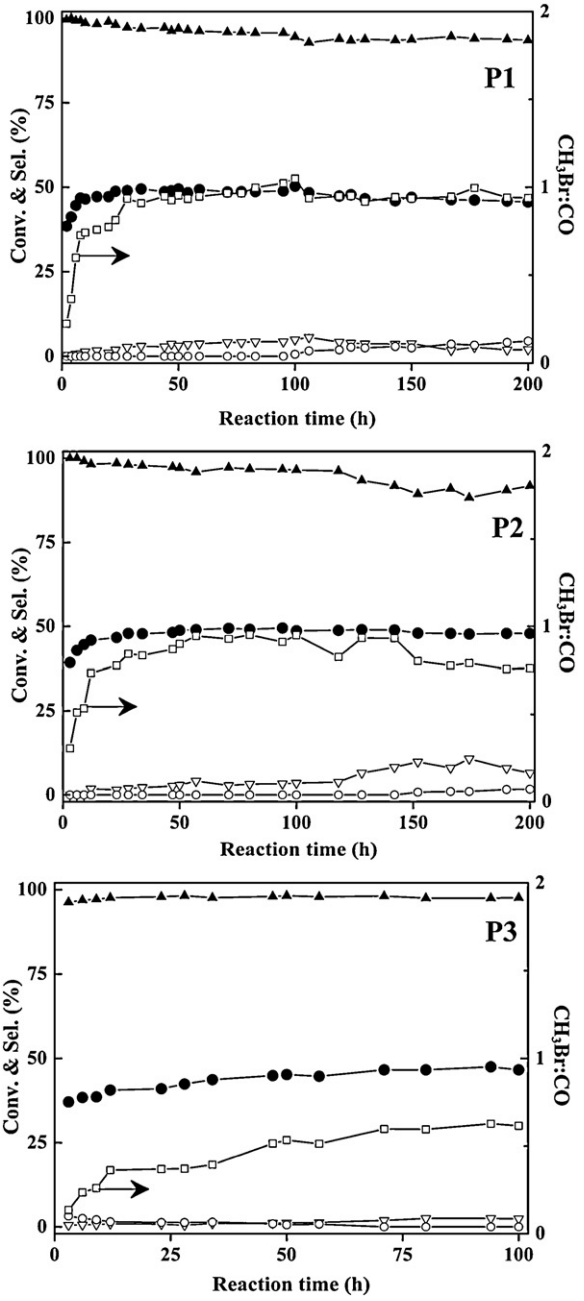


**Fig. 3.** Performances of the OBM reaction over different synthesized catalysts. Reaction conditions: *T* 570 °C, $CH_4$ 10 sccm, $O_2$ 5 sccm, 40 wt.% HBr/$H_2O$ 3.0 ml/h, catalyst 2.0 g. (●) $CH_4$; (▲) $CH_3Br$ + CO; (▽) $CH_2Br_2$; (◯) $CO_2$.

Generally, P1 and P2 showed similar OBM performances, but there are some small differences between them. Firstly, the reactivity of P1 showed a slight decline after 50 h while the reactivity of P2 was relatively stable, as reflected on the conversions of methane. Secondly, the total selectivity for $CH_3Br$ plus CO stayed above 95% and the ratio of $CH_3Br$:CO was close to 1.0 in the stable catalyst of P1. However, the total selectivity for $CH_3Br$ plus CO and the ratio

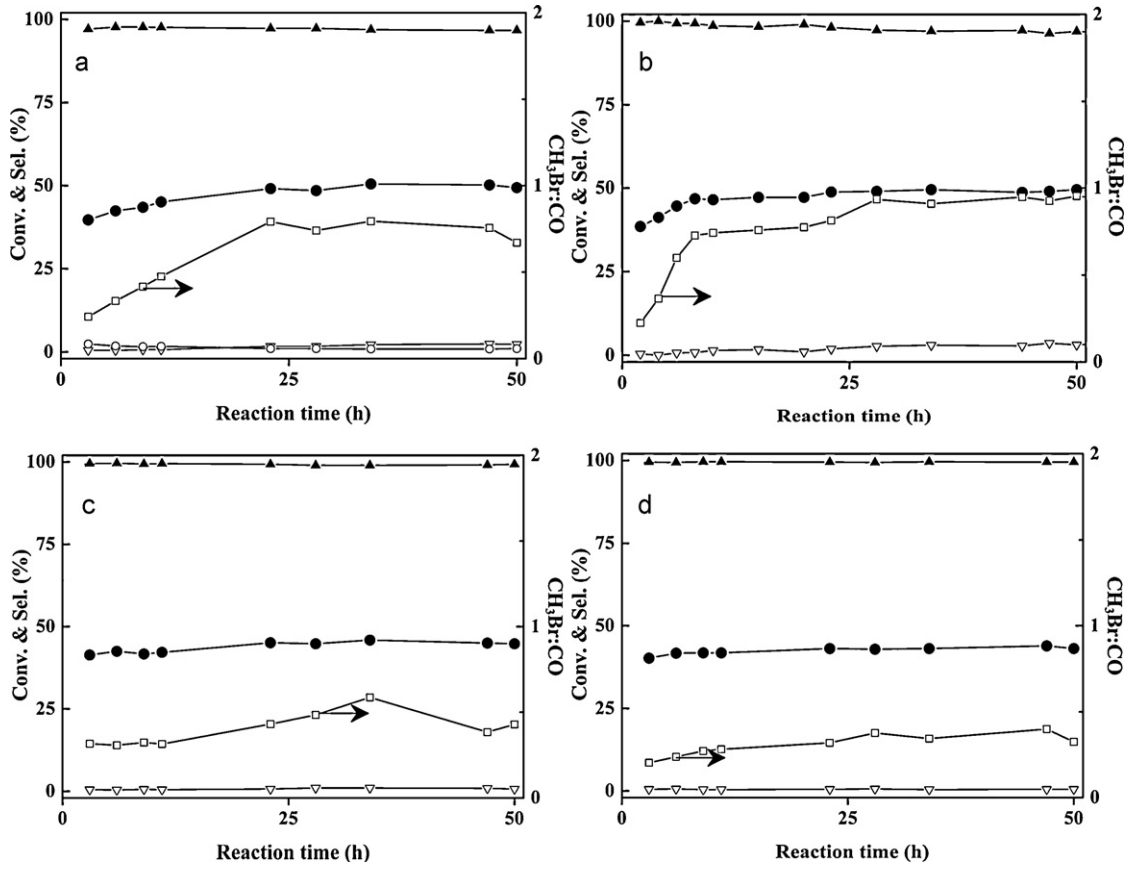


**Fig. 4.** Effect of $FePO_4$ loading on the OBM performance: (a) 5%, (b) 10%, (c) 20%, (d) 30%. Reaction conditions: $T$ 570 °C, $CH_4$ 10 sccm, $O_2$ 5 sccm, 40 wt.% $HBr/H_2O$ 3.0 ml/h, catalyst 2.0 g. (●) $CH_4$; (▲) $CH_3Br + CO$; (▽) $CH_2Br_2$; (◯) $CO_2$.

of $CH_3Br$:CO dropped gradually after 140 h for P2. Lastly, $CO_2$ was detected after about 100 h over P1, with the decline of $CH_2Br_2$ selectivity. Similar trends occurred over P2 at approximately 150 h. Coke deposition might be the cause of these changes in product distribution, as discussed later in Section 3.3. Obviously, the total selectivity for $CH_3Br$ plus CO and the ratio of $CH_3Br$:CO are relatively stable over P1. Since our aim products are equimolar $CH_3Br$ and CO, P1 was chosen for further investigation in the next part.

### 3.3. Effects of $FePO_4$ loading and reaction temperature

#### 3.3.1. Effect of $FePO_4$ loading

Fig. 4 presents the 50 h time-on-stream performances of the OBM reaction over the $FePO_4/SiO_2$ catalysts with different $FePO_4$ loadings. All the catalysts showed similar induction periods in the first 10 h. The induction period was even apparent when the loading was below 20%. Obviously, the induction periods were much shorter for the catalysts with high loading. It is interesting to notice that both the conversion of methane and the ratio of $CH_3Br$:CO reached maxima over the catalyst with 10 wt.% $FePO_4$ loading. When the loading was increased from 10% to 30%, the activity only declined slightly but the ratio of $CH_3Br$:CO dropped rapidly from 1.0 to 0.3. It has been revealed that $CH_3Br$ is the primary product, while $CH_2Br_2$ and CO are the secondary in the OBM system [15]. Since both $CH_3Br$ and CO are the main products of all these tests, the declined ratio of $CH_3Br$:CO with increasing $FePO_4$ loading demonstrated that more $CH_3Br$ was oxidized to CO in relatively higher loading.

Our previous report has revealed that the OBM reaction over iron phosphates followed a redox path [20]. Thus, it is speculated that the catalytic performances of different catalysts might be influenced by their redox abilities. Fig. 5 presents the $H_2$-TPR profiles of the $FePO_4/SiO_2$ catalysts with different $FePO_4$ loadings. Each sample showed a reduction peak at 380–550 °C that could be assigned to the reduction from $FePO_4$ to $Fe_2P_2O_7$ [23]. Besides, the summit temperature of each reduction peak shifted gradually from 462 to 502 °C when the loading of $FePO_4$ was increased from 5% to 30%, indicating the decline in redox abilities. The impacts of $FePO_4$ loading on the OBM performance might be attributed simply to two aspects: the amount of active sites and redox abilities. The increase in $FePO_4$ loading would increase the amount of active sites on one

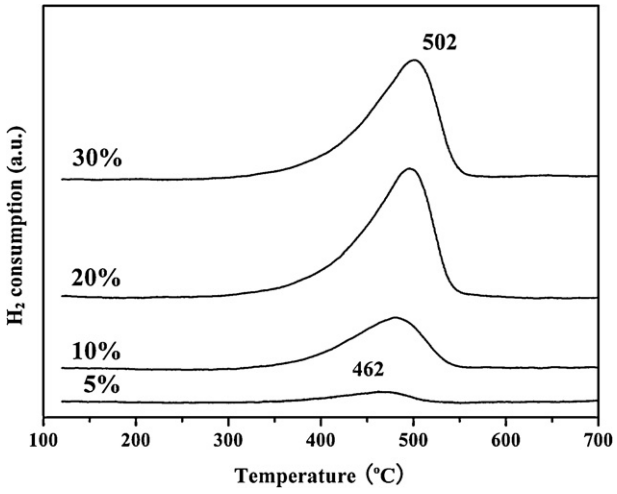


**Fig. 5.** $H_2$-TPR profiles of the synthesized catalysts with different loadings of $FePO_4$.

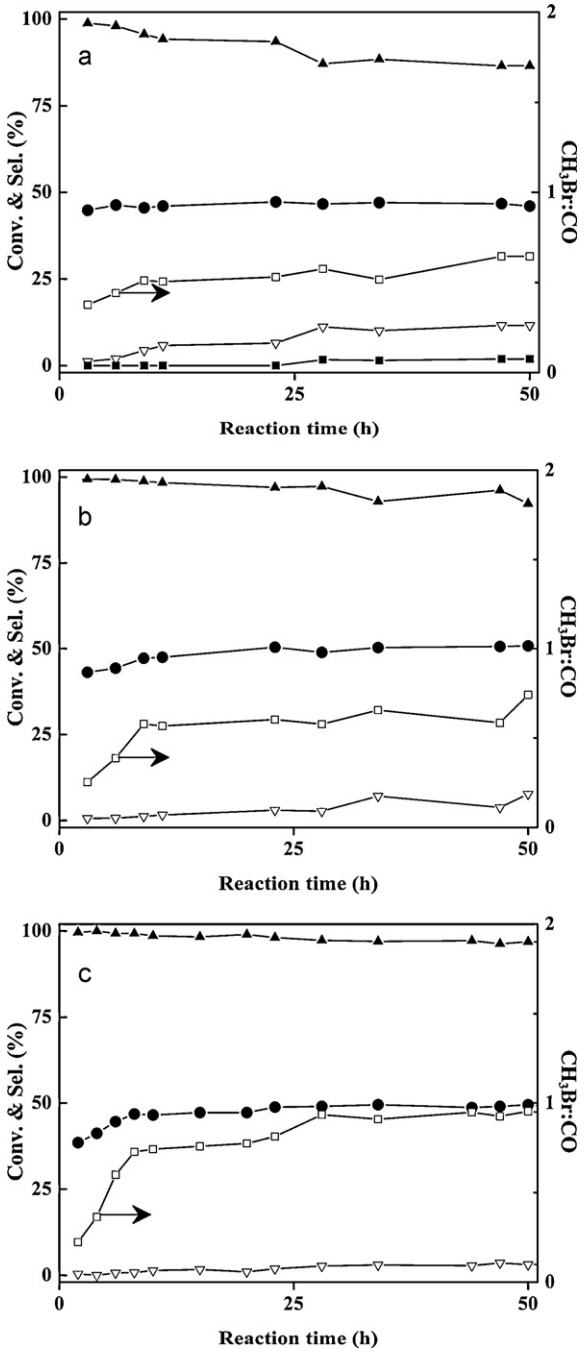


**Fig. 6.** Effect of reaction temperature on the OBM performance over P1: (a) 530 °C; (b) 550 °C; (c) 570 °C. Reaction conditions: $CH_4$ 10 sccm, $O_2$ 5 sccm, 40 wt.% HBr/$H_2O$ 3.0 ml/h, catalyst 2.0 g. (●) $CH_4$; (▲) $CH_3Br$ + CO; (▽) $CH_2Br_2$; (■) $CHBr_3$; (◯) $CO_2$.

hand and weakened the redox abilities on the other hand, leading to the maxima of methane conversion and the ratio of $CH_3Br$:CO.

### 3.3.2. Effect of reaction temperature

Fig. 6 shows the influence of reaction temperature on the OBM performances over P1. It is observed that the total selectivity for $CH_3Br$ plus CO and the ratio between them kept increasing when the reaction temperature was increased from 530 to 570 °C. But the effect of reaction temperature on methane conversion was almost negligible in the surveyed temperature range. Besides, the induction periods were not apparent at lower reaction temperatures. It is worthy to notice that small quantity of $CHBr_3$ was detected at 530 °C and the selectivity to $CH_2Br_2$ kept decreasing at elevated reaction temperatures. We have also investigated the reaction at higher temperatures ($T$ > 590 °C). In these cases, the selectivity to $CH_2Br_2$ was even lower but the ratio of $CH_3Br$:CO began to decline and $CO_2$ was produced immediately.

It is generally recognized that the OBM reaction was initiated by the formation of bromine radicals [15]. Thermodynamic analysis on the radical reactions between methane and bromine has revealed that $CH_2Br_2$ formation become non-spontaneous above 450 °C [5]. Thus, the selectivity to $CH_2Br_2$ could be restricted by conducting the OBM reaction at relatively higher reaction temperatures, as confirmed by our experiments. On the other hand, the poor product distributions in lower reaction temperatures suggested that the catalysts employed in the present system are not as selective as electrophilic super-acid catalysts. However, equimolar $CH_3Br$ and CO are attainable in the present catalytic system by manipulating the reaction temperature.

## 3.4. Coke deposition

### 3.4.1. Regeneration of the used catalysts

In Section 3.2, the long-term stability experiment of P1 catalyst was studied. The conversion of methane declined slightly after 50 h and the selectivity to $CO_2$ increased gradually after 100 h. These facts indicated that coke deposition might occur. To elucidate this point, the used catalyst was regenerated in situ in a flow of 33.3 vol.% $O_2/N_2$ (15 sccm) at 570 °C overnight. The OBM reaction was then re-conducted over this regenerated sample for another 100 h at the same reaction conditions. As we have expected, the conversion of methane increased gradually in the first 20 h, indicating the partial recovery of activity. Besides, a similar induction period was observed, with the increase of both methane conversion and the ratio of $CH_3Br$:CO. Unfortunately, the conversion of methane still showed a slight decline after a short induction period, together with the increase of $CO_2$ selectivity.

### 3.4.2. Structural analysis

In order to ascertain the structural properties of P1 during the OBM reaction, the samples after different reaction times were also investigated by $N_2$-adsorption and FTIR techniques. The corresponding physical properties of P1 for different reaction times are presented in Table 1. It is obvious that the pore structure properties between P1-100 and the fresh sample showed little differences. The surface area was a little higher for the fresh sample. Surprisingly, the surface area of P1-300 was only 36 $m^2/g$, which reduced by one magnitude as compared with that of the fresh sample. Serious coke deposition might occur on the silica carrier, leading to the block of mesopores and drastic reduction in surface areas. The transmission IR spectra of P1 for different reaction times are also presented in Fig. 1. It is observed that the spectra between P1-100 and the fresh sample are very close, thus the functional groups in the fresh sample might be well-reserved after reacted for 100 h. However, the spectrum of P1-300 is very different from that of the fresh sample. The peaks at 1638 and 809 $cm^{-1}$, corresponding to the vibrations of surface OH and P–O–P groups, disappeared in this sample. It has been reported that the P–O–P bridges may transform easily and reversibly to surface hydroxyl groups through Eq. (4) [22]. By far, the active sites for coke deposition could not be well assigned yet. It is speculated that surface dehydration process would be facilitated by serious coke deposition, resulting in the broken of the P–O–P bridges.

$$\text{P–O–P} + H_2O \leftrightarrow 2\text{P–OH} \quad (4)$$

### 3.4.3. TPO

Fig. 7 shows the TPO profiles of P1-300. There was a huge $O_2$ consumption peak in the temperature range between 500 and 800 °C.

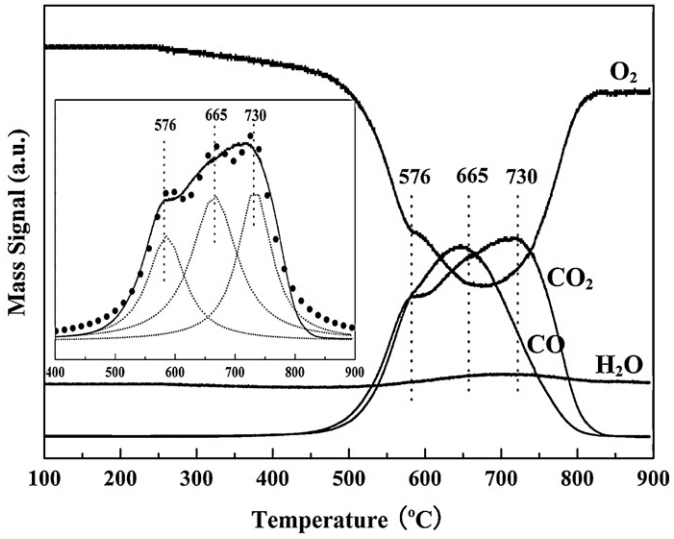


**Fig. 7.** TPO-MS profiles of P1-300. Inset is the fitting of $CO_2$ signal.

Besides, CO and $CO_2$ were detected simultaneously with the consumption of $O_2$. The experiment confirmed further that the catalyst suffered serious coke deposition. The $CO_2$ signal could be fitted into three peaks and the summit temperatures of each peak were 576, 665 and 730 °C, respectively (inset in Fig. 7). Therefore, there should be at least three different types of carbonaceous species depositing on P1-300. It was noticed that a weak signal of $H_2O$ was also detected. The huge contrast in the mass signal intensity between $CO_2$ and $H_2O$ indicated that the deposited carbonaceous species had a high ratio of C/H. In Section 3.3.1, $CO_2$ was produced rapidly on the regenerated catalyst. Since the regeneration temperature of the used catalyst was only 570 °C, which was far lower than the burning temperatures of the deposited cokes. Hence, the rapid production of $CO_2$ on the regenerated catalyst might be resulted from partial removal of the depositing cokes.

*3.4.4. Insight into coke deposition*

The textural analysis of P1 after different reaction times by $N_2$-adsorption has indicated that serious coke formation might block up the mesopores in the silica carrier, leading to drastic decline in surface areas. Hence, it is likely that cokes deposited on the pores of silica during the reaction. It has been demonstrated that the stable active components of iron phosphate catalysts comprised of near-equimolar $\alpha$-$Fe_3(P_2O_7)_2$ and $Fe_2P_2O_7$ [20]. The slight deactivation of the iron phosphate catalysts during the reaction might be related to the broken of the P–O–P bridges in $P_2O_7^{2-}$ groups. It was observed that the selectivity to $CO_2$ increased simultaneously with the decrease of $CH_2Br_2$ selectivity both on the fresh sample and on the regenerated one, but the total selectivity for $CH_3Br$ plus CO stayed relatively stable. Therefore, the formation of $CO_2$ could be deemed as an indication of coke deposition. The changes in product distribution suggested that the deposited cokes might be resulted from the accumulation of $CH_2Br_2$. In an earlier literature, Lorkovic et al. [11] found that adsorbed carbon and aromatics were significantly lower with pure $CH_3Br$ than a feed of mixed bromomethanes when condensed over CaO/zeolite composites. TPO experiments on P1-300 have indicated that the depositing cokes had a high ratio of C/H, which is in accord with the report by Lorkovic et al. [11].

## 4. Conclusions

Three different kinds of $FePO_4/SiO_2$ catalysts have been synthesized and used for the oxy-bromination of methane reaction. All these samples showed very stable performances. The influences of $FePO_4$ loading and reaction temperature on the catalytic performance have been investigated. A maximum methane conversion of about 50% and near-equimolar $CH_3Br$ and CO were achieved over the $FePO_4/SiO_2$ catalyst with 10% loading at 570 °C. The low temperature performance of the sample revealed that the catalytic system was not selective, but the ratio between $CH_3Br$ and CO could be adjusted easily by manipulating the reaction parameters. Coke deposition occurred over the catalyst after a long running period, with a slight decline in activity. Characterization results from $N_2$-adsorption, FTIR and TPO suggested that the accumulation of $CH_2Br_2$ during the reaction could be the direct cause of coke formation. These findings would be beneficial for the design of iron phosphate catalysts with superior catalytic performance for the OBM reaction.

## Acknowledgement

This work was financially supported by the Ministry of Science and Technology of China (2005CB221406).

## References

[1] R.H. Crabtree, Chem. Rev. 95 (1995) 987.
[2] J.H. Lunsford, Catal. Today 63 (2000) 165.
[3] S. Romanow, Hydrocarbon Process. 80 (2001) 11.
[4] B. Vora, J.Q. Chen, A. Bozzano, B. Glover, P. Barger, Catal. Today 141 (2009) 77.
[5] V. Degirmenci, D. Uner, A. Yilmaz, Catal. Today 106 (2005) 252.
[6] A.J. Rouco, J. Catal. 157 (1995) 380.
[7] E. Peringer, S.G. Podkolzin, M.E. Jones, R. Olindo, J.A. Lercher, Top. Catal. 38 (2006) 211.
[8] G.A. Olah, Acc. Chem. Res. 20 (1987) 422.
[9] V. Degirmenci, A. Yilmaz, D. Uner, Catal. Today 142 (2009) 30.
[10] D.Z. Zhang, Y.X. Wei, L. Xu, A.P. Du, F.X. Chang, B.L. Su, Z.M. Liu, Catal. Lett. 109 (2006) 97.
[11] I.M. Lorkovic, M. Noy, M. Weiss, J. Sherman, E. Mcfarland, G.D. Stucky, P.C. Ford, Chem. Commun. 5 (2004) 566.
[12] X.P. Zhou, A. Yilmaz, G.A. Yilmaz, I.M. Lorkovic, L.E. Laverman, M. Weiss, J.H. Sherman, E.W. Mcfarland, G.D. Stucky, P.C. Ford, Chem Commun. 18 (2003) 2294.
[13] I.M. Lorkovic, A. Yilmaz, G.A. Yilmaz, X.P. Zhou, L.E. Laverman, S. Sun, D.J. Schaefer, M. Weiss, M.L. Noy, C.I. Cutler, J.H. Sherman, E.W. Mcfarland, G.D. Stucky, P.C. Ford, Catal. Today 98 (2004) 317.
[14] A. Breed, M.F. Doherty, S. Gadewar, P. Grosso, I.M. Lorkovic, E.W. Mcfarland, Catal. Today 106 (2005) 301.
[15] K.X. Wang, H.F. Xu, W.S. Li, X.P. Zhou, J. Mol. Catal. A: Chem. 225 (2005) 65.
[16] K.X. Wang, H.F. Xu, W.S. Li, C.T. Au, X.P. Zhou, Appl. Catal. A: Gen. 304 (2006) 168.
[17] Z. Liu, L. Huang, W.S. Li, F. Yang, C.T. Au, X.P. Zhou, J. Mol. Catal. A: Chem. 273 (2007) 14.
[18] Y.F. Fan, D. Ma, X.H. Bao, Catal. Lett. 130 (2009) 286.
[19] R. Lin, Y. Ding, L. Gong, J. Li, W. Chen, L. Yan, L. Yuan, Appl. Catal. A: Gen. 353 (2009) 87.
[20] R. Lin, Y. Ding, L. Gong, W. Dong, J. Wang, T. Zhang, J. Catal. 272 (2010) 65.
[21] P. Bonnet, J.M.M. Millet, C. Leclercq, J.C. Védrine, J. Catal. 158 (1995) 128.
[22] G.O. Alptekin, A.M. Herring, D.L. Williamson, T.R. Ohno, R.L. McCormick, J. Catal. 181 (1999) 104.
[23] X. Wang, Y. Wang, Q. Tang, Q. Guo, Q. Zhang, H. Wan, J. Catal. 217 (2003) 457.